

Electrical and dielectric behavior of the system $\text{Gd}_{1-x}\text{Ba}_x\text{CoO}_3$ ($x = 0.00, 0.10, 0.20$) synthesized by chemical route

K. D. Mandal^{*1}, L. Behera¹, R. L. Prasad¹, and R. C. Behera²

¹ Department of Chemistry, North Eastern Regional Institute of Science & Technology, Nirjuli, Itanagar – 791109, Arunachal Pradesh, India

² Department of Metallurgical Engineering, Regional Engineering College, Rourkela-769008, Orissa, India

Received 7 June 2002, revised 27 August 2002, accepted 17 February 2003

Published online 15 June 2003

Key words gadolinium cobalt oxide, perovskite oxides, chemical synthesis, electrical transport, dielectric response.

PACS 72.20.-i

The samples in the system $\text{Gd}_{1-x}\text{Ba}_x\text{CoO}_3$ ($x = 0.00, 0.10, 0.20$) were prepared by chemical route. These samples form single-phase materials, which were confirmed by XRD and TGA studies. The presence of interfacial polarization is responsible for high value of dielectric constant in these materials. The conductivity observed in $\text{Gd}_{1-x}\text{Ba}_x\text{CoO}_3$ system may be due to mobile holes created by excitation of an electron from the π^* band to an acceptor level.

1 Introduction

The perovskite oxide is a field of great interest for Material Scientists. A number of perovskite oxides have been studied by various groups of workers [1,2,3]. Perovskite oxides have been studied extensively because of their technological applications. The reason for broad application includes their stability over wide temperature ranges and their low cost and ease with which composition and microstructure may be optimized and tailored to specific applications [4,5,6]. Rare earth cobaltates show interesting electrical and magnetic properties. The properties of those materials depends on spin state and valance state of transition metal ions and ionic radii of rare earth ions [7].

We have been studying electrical and dielectric properties of perovskite oxides and valance compensated perovskite oxides [8,9,10,11] which were synthesized by conventional ceramic method. Recently we have taken up few systems of perovskite oxides, which were synthesized by chemical route and published elsewhere [10,12]. In this paper we report the method of synthesis of the $\text{Gd}_{1-x}\text{Ba}_x\text{CoO}_3$ ($x = 0.00, 0.10, 0.20$) system by the chemical route and study the electrical and dielectric properties. The change in electrical and dielectric properties in the system with doping of Ba^{+2} ions is also explained.

2 Experiment

Compositions with $x=0.00, 0.10, 0.20$, in the system $\text{Gd}_{1-x}\text{Ba}_x\text{CoO}_3$ were prepared by chemical method using Citric acid. All chemicals used in this method has purity 99.9% or betters. Gadolinium Oxide, Cobalt (II) nitrate and Barium nitrate were used as starting materials.

Gadolinium oxide was converted into nitrate by adding conc. HNO_3 and evaporated to dryness. Standard solution of metal nitrate was prepared in distilled water. Solution having stoichiometric amount of those

* Corresponding author: e-mail: kdm@nerist.ernet.in

metallic ions in the system $Gd_{1-x}Ba_xCoO_3$ ($x = 0.00, 0.10, 0.20$) were mixed in a beaker. Calculated amount of Citric acid equivalent to the metals ions is added to the solution. The solution was mixed on a hot plate magnetic stirrer and warmed up to 60-70° C and kept the temperature constant till total evaporation of water. The residue was dried at 60° – 70° C in a hot air oven for 24 hrs. Dry powder was calcined at 600° C for 8hrs. The calcined powder was grounded into fine powder and made cylindrical pellets. The pellets were sintered at 650° C for 6 hrs. The X-ray diffraction patterns of fine calcined powder were recorded ($2\theta = 10-90^\circ$) on Philips Analytical X-ray diffractometer using $Cu-K_\alpha$ radiations.

The DC electrical resistance (R) of the sintered pellets coated with silver paint was measured with variation of temperature using a Keithley electrometer. The specific conductance of the sample was calculated using the formula $\sigma = d / RA$ where d & A are the thickness and cross section area of flat surface of the pellet respectively. The capacitance (C) was measured using a 3532 LCR HiTESTER (HIOKI) with the variation of frequency and temperature. The relative dielectric constant (ϵ_r) of the materials was calculated by the formula given below:

$$\epsilon_r = C d / \epsilon_0 A \quad (1)$$

where d and A are the thickness and cross section area of flat surface of the pellet respectively and ϵ_0 is permittivity of free space (8.85×10^{-12}). The thermal decomposition (TGA-DTA) for dried sample of $Gd_{1-x}Ba_xCoO_3$ ($x = 0.10$) was recorded on Delta Series TGA7 in air.

3 Result and discussion

Compositions $x = 0.00, 0.10, 0.20$ synthesized in the system $Gd_{1-x}Ba_xCoO_3$ were found to be single-phase materials. X-ray diffraction data (observed & calculated), relative intensity and h k l value for the system $Gd_{0.9}Ba_{0.1}CoO_3$ is given in Table 1. X - ray data of the samples were indexed on the basis of a orthorhombic unit cell similar to $GdCoO_3$. The crystal system, lattice parameter, unit cell volume, dielectric constant and DC conductivity for different composition is calculated and given in Table 2. The recorded peaks were sharp and strong enough to confirm high crystallinity of the synthesized sample. The cell parameters and unit cell volume (V) of $Gd_{1-x}Ba_xCoO_3$ increases with increase in Ba^{+2} ions concentration. This is may be due to large ionic radius of Ba^{+2} ion (1.42\AA), which when substituted at A- site and displaces smaller Gd^{+3} ions (1.06\AA) [13].

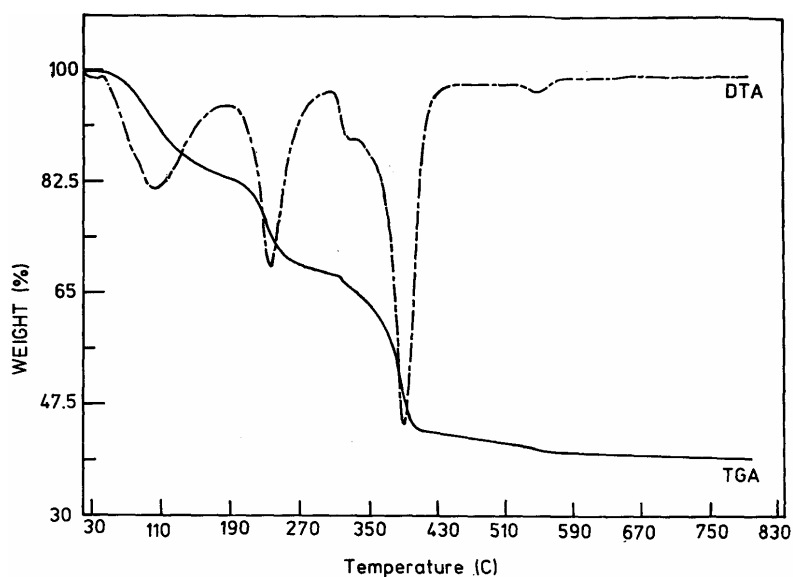
Table 1 X-ray diffraction data (observed & calculated), relative intensity and h k l value for the system $Gd_{1-x}Ba_xCoO_3$ ($x = 0.10$).

hkl	2 θ	2 θ_{cal}	D-2 θ	d(\AA)	d(\AA)cal	D-d(\AA)	I/I _o
111	23.8759	23.9235	-0.0476	3.7239	3.7166	0.0073	100
300	30.3876	30.2448	0.1428	2.9391	2.9527	-0.0136	44
121	34.3308	33.7781	0.5527	2.6100	2.6515	-0.0414	31
012	36.6460	36.8948	-0.2488	2.4503	2.4343	0.0160	33
212	42.0126	42.3331	-0.3205	2.1488	2.1333	0.0155	37
130	42.9576	42.5910	0.3666	2.1037	2.1210	-0.0173	19
321	44.8866	44.7486	0.1380	2.0177	2.0236	-0.0059	38
131	46.8148	46.1283	0.6864	1.9390	1.9662	-0.0272	32
222	49.2355	48.9778	0.2577	1.8492	1.8583	-0.0091	5
023	59.5674	59.9298	-0.3625	1.5508	1.5422	0.0085	6
340	65.0147	65.0519	-0.0372	1.4334	1.4326	0.0007	8
042	67.9686	67.3386	0.6300	1.3781	1.3894	-0.0114	6
133	69.5147	69.6481	-0.1334	1.3512	1.3489	0.0023	9
251	77.8281	78.1361	-0.3079	1.2263	1.2222	0.0041	5
134	86.5339	87.3817	-0.8478	1.1239	1.1151	0.0087	2
ST-DEV=	0.1101	0.0043					

Table 2 Composition, structure, lattice parameters, Unit Cell volume, dielectric constant and DC conductivity for the system $Gd_{1-x}Ba_xCoO_3$

Composition	Structure	Lattice parameter (Å)	Unit Cell volume (Å ³)	Dielectric constant at 1kHz & 500K	DC conductivity(σ) at 400K($\Omega^{-1} \text{cm}^{-1}$)
x = 0.00	orthorhombic	a=5.2032 b=5.3935 c=7.4817	209.9625	2678	3.5931X 10 ⁻³
x = 0.10	orthorhombic	a=8.8580 b=6.5536 c=5.2438	304.4138	7353	3.17125X 10 ⁻²
x = 0.20	orthorhombic	a=8.8864 b=6.5397 c=5.2593	305.6402	24158	8.1024X 10 ⁻³

The thermal decomposition (TGA-DTA) of dried prepared sample yield $Gd_{1-x}Ba_xCoO_3$ ($x = 0.10$) perovskite phase as the end product preceded by the formation of four different stable intermediate which is shown in Fig.1. At temperature $T < 207^\circ\text{C}$ there is a 17.67% mass loss which is caused by removal of the surface and occluded water and excess of Citric acid present in the sample. The intermediate products are stable over a very limited temperature interval and are difficult to delineate from a normal TG curve. A differential thermogravimetric (DTA) curve consists of the plot of $d(\Delta m)/dT$ i.e. the rate of mass change with respect to temperature versus temperature is shown in the same figure. The area under the DTA peak provides the measure of the total mass change in a given step. The DTA curve facilitates better resolution of the weakly stable intermediate which was found around 300°C & 550°C . The solid solution of $Gd_{0.9}Ba_{0.1}CoO_3$ is formed at 575°C which is less as compared to the conventional ceramic method.

**Fig. 1** TGA and DTA plots for the sample $Gd_{0.9}Ba_{0.1}CoO_3$.

Plots of ϵ_r versus temperature for compositions $x = 0.00, 0.10, 0.20$ at 100 Hz and 1kHz are shown in Fig.2 and Fig.3 respectively. At 100 Hz the dielectric constant is high for all the samples. A sharp peak is observed at 375 K for the composition $x = 0.10$ at both frequencies (100Hz and 1kHz) which is characteristic of ferroelectric to paraelectric transition. The transition temperature remains same (375 K) at two frequencies. The sharpness of ferroelectric to paraelectric transition may be due to large grain size. The intensity of peak at 1kHz is very high. Peaks are also observed in the dielectric constant (ϵ_r) versus temperature plot for the composition $x = 0.00$ and 0.30 at 1kHz but they are diffused type. The dielectric constant for the composition x

= 0.10 shows the constant value beyond 400 K. At 100 Hz, the ϵ_r of $GdCoO_3$ increases slowly with temperature whereas a rapid increase in dielectric constant is observed for the composition $x = 0.20$. At 1 kHz the ϵ_r for $x = 0.00$, 0.10 show constant value after 400 K whereas a peak may be observed near 500 K for the sample $x = 0.20$. The peaks dielectric constant for the sample $x = 0.20$ are 4×10^5 and 1×10^5 at 100 Hz and 1 kHz respectively. At 100 Hz, the dielectric constant for the composition $x = 0.30$ is continuously increasing with temperature. At 500 K, the ϵ_r for $x = 0.30$ is observed 12×10^5 . The variation in dielectric constant with temperature decreases with increasing frequency. The dielectric constant of these materials increases with increasing of Ba^{2+} ions concentration in the system. This is due to the vacancy created in oxygen sites as $Gd_{1-x}Ba_xCoO_{3-x/2}$.

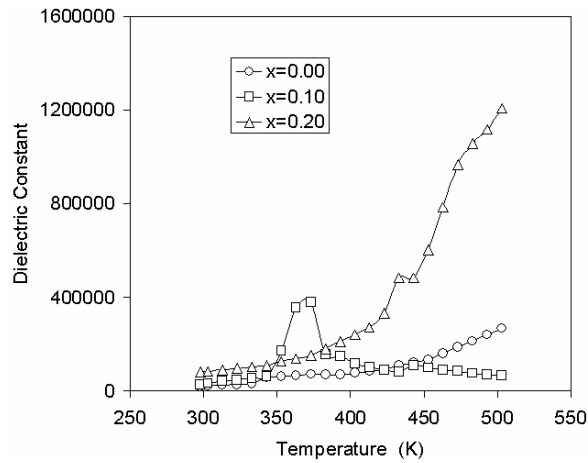


Fig. 2 Plots of dielectric constant vs temperature at 100 Hz for the system $Gd_{1-x}Ba_xCoO_3$.

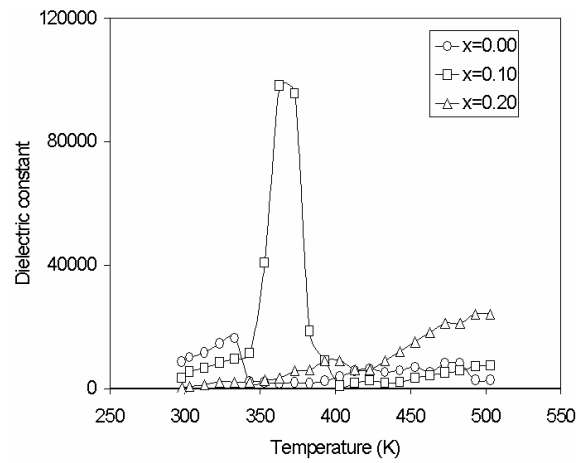


Fig. 3 Plots of dielectric constant vs temperature at 1 kHz for the system $Gd_{1-x}Ba_xCoO_3$.

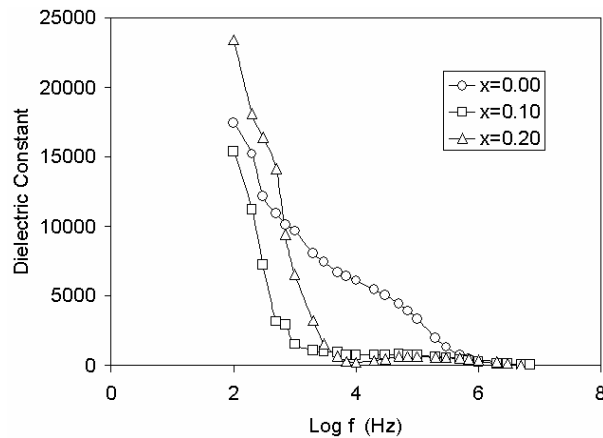


Fig. 4 Plots of Dielectric Constant vs log f (Hz), for the system $Gd_{1-x}Ba_xCoO_3$ at 300K.

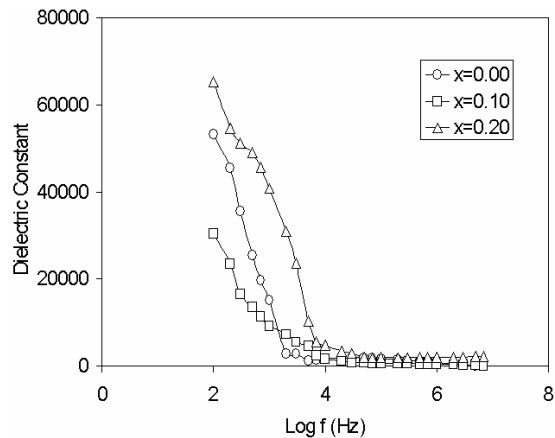


Fig. 5 Plots of Dielectric Constant vs log f for the system $Gd_{1-x}Ba_xCoO_3$ at 400K.

On temperature variation, the crystallographic dimensions change due to distortion of the octahedra. As a result, the distorted octahedra are coupled together and a very large spontaneous polarization can be achieved at the transition temperature. This large spontaneous polarization will lead to high dielectric constant observed for the samples $x = 0.10$ and 0.20 .

The plots of frequency variation of dielectric constant at two temperatures 300 and 400 K are shown in Fig.4 and Fig.5 respectively for the compositions $x = 0.00, 0.10, 0.20$. These samples show a decreasing trend in the values as the frequency is increased which is the normal behavior of ferrimagnetic materials [14, 15]. The dielectric dispersion is sharp initially and the ϵ_r values decrease with increase in frequency followed by a frequency independent behavior. The normal dielectric behaviour of spinel ferrites was explained by Maxwell- Wagner interfacial type polarization, which is in agreement with Koops theory [16]. Iwachi [17] gave a strong correlation between conduction mechanism and the dielectric behavior of the samples. The variation of dielectric constant with frequency and temperature show the presence of interfacial polarization in these materials. This interfacial polarization arises due to compositional fluctuation, which are due to random occupation of Ba^{+2} ions in octahedral and dodecahedral sites.

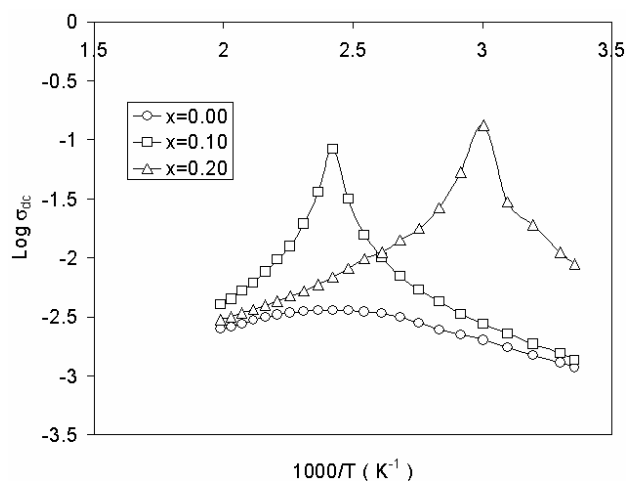


Fig. 6 Plots of $\text{Log } \sigma_{dc}$ vs $1000/T$ for the system $\text{Gd}_{1-x}\text{Ba}_x\text{CoO}_3$.

Plots of $\log \sigma_{dc}$ Vs $1000/T$ for compositions $x = 0.00, 0.10, 0.20$ in the system $\text{Gd}_{1-x}\text{Ba}_x\text{CoO}_3$ are shown in Fig.6. Two intense peaks are observed for the compositions $x = 0.10$ and 0.20 . A defused peak is also observed in the case of GdCoO_3 . All three samples under investigation show similar DC conductivity behavior. For composition $x = 0.00$, the conductivity increase till 400 K and then decrease with increase in temperature. But in the case of compositions $x = 0.10$ & 0.20 , the conductivity increases up to 323 K and 333 K respectively then decreases with increase temperature. All the three compositions show semiconducting behavior at low temperature and metallic behavior at high temperature. It is also observed that the conductivity of the system increases on increasing of Ba^{2+} ions concentration. The variation in conductivity shows interesting insulator-metal phase transition with increasing temperature. The d-d coulomb interaction energy U and d-band width w dominated the electronic structure near the Fermi level. If $U > w$ it is an insulator with a gap between the conductivity and valence bands determined by the energy required for fluctuations [18]. In the case of $U < w$ it is a metal without a gap. From experimental results, it was found that GdCoO_3 is so-called Mott insulator. The conductivity observed in $\text{Gd}_{1-x}\text{Ba}_x\text{CoO}_3$ may be due to mobile holes created by excitation of an electron from the π^* band to an acceptor level. As the amount of Ba substitution is increased, the acceptor orbital interact to form an impurity band. If the high and low spin states have comparable energies, the formation of impurity bands generate a spontaneous ferromagnetism, wherein the σ^* bands of up-spin overlap the π^* band of down-spin. The transport properties of $\text{Gd}_{1-x}\text{Ba}_x\text{CoO}_3$ is explained by the complicated Co-3d band structure [19]. The highest occupied molecular orbital contained Co-3d and O-2p orbitals. The insulator-metal transition, which appears at high temperatures, is not a Mott-Hubbard transition but a charge-transfer type transition. The spin state transition occurs mainly due to the variation of the Co-O bond length with increasing of temperature. The transition occurs through the interaction between the 2p orbitals or the Co-3d and O-2p orbitals. $\text{Gd}_{1-x}\text{Ba}_x\text{CoO}_3$ is nearly intermediate between Mott-Hubbard type compound and charge transfer- type compounds with interaction between Co and O ions with valance and conductivity bands consisting of strongly mixed O-2p and Co-3d bands because of the electronic correlation [20]. The covalence of $\text{Gd}_{1-x}\text{Ba}_x\text{CoO}_3$ is due to the main

contribution of the hybridization between Co and O orbital. An increase of the Co-O bond length causes the low-spin state gradually to become unstable, while the high-spin state becomes stable. There is possibility of existence of an intermediate spin state. The insulator-metal transition occurs due to the interaction between mixed states consisting of electrons for Co ions and holes for O ions.

Acknowledgement Authors are grateful to Council of Scientific and Industrial Research, New Delhi for financial assistance.

References

- [1] P. Raccach and J. B. Goodenough, *Phys. Rev.* **155**, 932 (1967).
- [2] Om. Prakash, L. Pandey, M. K. Sharma, and D. Kumar, *J. Mater. Sci.* **24**, 4505 (1989).
- [3] A. J. Mountwala, *J. Amer. Ceram. Soc.* **54**, 544 (1971).
- [4] R. C. Buchanan, *Ceramic Materials for Electronics*, Marcel Dekker, New York 1986
- [5] A. Halliyal, U. Kumar, R. E. Newnham, and L. E. Cross, *J. Am. Ceram. Soc.* **70**, 119 (1987).
- [6] B. Jaffe, W. R. Cook Jr., and H. Jaffe, *Piezoelectric Ceramics*, Academic Press, London 1971.
- [7] C. N. R. Rao, V.G. Bhide, and N. F. Mott, *Philos. Mag.* **32**, 1277 (1975).
- [8] Om Parkash, K. D. Mandal, and S. Sastry Mandalika, *J. Alloys and Compounds* **228**, 177 (1995).
- [9] K. D. Mandal, M. S. Sastry, and Om Parkash, *J. Mater. Sci.* **14**, 1412 (1995).
- [10] K. D. Mandal and Om Parkash, *Cryst. Res. Technol.* **31**, K36 (1996).
- [11] K. D. Mandal, C. C. Christopher, M. S. Sastry, D. Kumar, and Om Parkash, *J. Mater. Science* **31**, 4705 (1996).
- [12] K. D. Mandal, L. Behera, and K. Ismail, *J. Alloys and Compounds* **325**, L17 (2001).
- [13] R. D. Shannon and C. T. Prewitt, *Acta Cryst.* **B25**, 925 (1969).
- [14] S. S. Suryavanshi, R. S. Patil, S. A. Patil, and S. R. Sawant, *J. Less Common Metals* **168**, 169 (1991).
- [15] S. S. Bellad, S. C. Watawe, and B. K. Chougule, *Mater. Res. Bull.* **34**, 1099 (1999).
- [16] C.G. Koops, *Phys. Rev.* **83**, 121 (1951).
- [17] K. Iwachi, *Jpn. J. Appl. Phys.* **10**, 1520 (1971).
- [18] Takahashi Hidekazu, Munakata Fumio, and Yamanaka Mitsugu, *Phys. Rev.* **B 57**, 15211 (1998).
- [19] M. A. Senaris- Rodriguez and J. B. Goodenough, *J. Solid state Chem.* **116**, 224 (1995).
- [20] T. Mizokawa and A. Fujimori, *Phys. Rev.* **54**, 5368 (1996).